JOURNAL OF AGRICULTURAL AND FOOD CHEMISTRY

Ethyl Hexanoate Transfer Modeling in Carrageenan Matrices for Determination of Diffusion and Partition Properties

ALEXANDRE JUTEAU-VIGIER,† SAMUEL ATLAN,† ISABELLE DELERIS,† ELISABETH GUICHARD,‡ ISABELLE SOUCHON,† AND IOAN CRISTIAN TRELEA*,†

UMR 782 Génie et Microbiologie des Procédés Alimentaires, AgroParisTech, INRA, BP01, 1 Avenue Lucien Brétignières, F-78850 Thiverval-Grignon, France, and UMR 1129 Flaveur, Vision et Comportement du Consommateur, CHU de Bourgogne, ENESAD, INRA, Université de Bourgogne, F-21065 Dijon Cedex, France

Aroma compound properties in food matrices, such as volatility and diffusivity, have to be determined to understand the effect of composition and structure on aroma release and perception. This work illustrates the use of mass transfer modeling to identify diffusion and partition properties of ethyl hexanoate in water and in carrageenan matrices with various degrees of structure. The comparison of results obtained with a diffusive model to those obtained with a convective model highlights the importance of considering the appropriate transfer mechanism. Modeling of the preliminary experimental steps ensures correct estimation of the conditions for the main aroma release step. The obtained values of partition and diffusion coefficients are in agreement with those found in the literature (either experimentally determined or predicted by theoretical equations) and demonstrate that the structure level of carrageenan matrices has little influence on diffusion properties of ethyl hexanoate (less than 20%).

KEYWORDS: Aroma release; modeling; partition coefficient; mass transfer; convection; diffusion coefficient; volatile compound

INTRODUCTION

To induce aroma perception, odorant volatile molecules must be released from food matrices and then transported to the olfactory receptors. However, it is well-known that changes in both food composition (*1*) and structure (*2*, *3*) often lead to a modified aroma perception that could be explained by sensory interactions (*4*, *5*) but also by the release from food matrices (*6*, *7*). To clarify the sensory and/or physicochemical nature of the effect of the food structure on aroma perception, it is necessary to determine the relevant physicochemical properties of aroma compounds in food matrices in order to better quantify the physical mechanisms explaining aroma release.

Static headspace methods are widely used in aroma studies for volatile release quantification. When performed at the thermodynamic equilibrium, a partition coefficient between the gas phase and the food matrix can be calculated, providing quantitative information on the retention of aroma compounds by the food matrix.

However, aroma release and perception are time-dependent phenomena, and partitioning is not a sufficient key for an overall understanding of the behavior of volatiles in food matrices (*8*). Several approaches have been developed to obtain the kinetic parameters of aroma release, depending on the experimental systems. The measurements can be performed under in vivo (*9*, *10*) or in vitro conditions (*11*, *12*). In vitro experimental systems can be open systems with a constant gas flow diluting the gas phase above the sample (*13*) or closed systems (equilibrium establishment) (*14*).

Numerous volatile time−release curves were obtained from model or real food matrices, from monophasic or multiphasic systems, and from liquid, thickened, or gelled matrices. A descriptive analysis of these kinetic curves is often made without modeling of the release, which could provide information on mechanisms involved (diffusion or convection, for example) and/or on the limiting step in the mass transfer. Several modeling approaches have been considered in the literature (*15*), however. Data-driven models consist of mathematical functions that best describe the release curves (*16*, *17*), but no real description of the release mechanisms can be obtained in this way. The information obtained cannot be used for other kinetic predictions.

The use of a mechanistic description (*13*, *18*) is more appropriate to determine aroma compound properties and to identify the limiting step in the mass transfer. Depending on the experimental setup and on the hydrodynamic conditions, two main mass transfer mechanisms have to be considered (*19*): convective transport when phases are well-stirred (**Figure 1a**) and diffusive transport when they are not

* To whom correspondence should be addressed. Tel: +33 13081 5490. Fax: +33 13081 5597. E-mail: cristian.trelea@agroparistech.fr.
† UMR 782 Génie et Microbiologie des Procédés Alimentaires.
‡ UMR 1129 Flaveur, Vision et Comportement du Consommateur.

10.1021/jf0626415 CCC: $37.00
Published on Web 04/10/2007

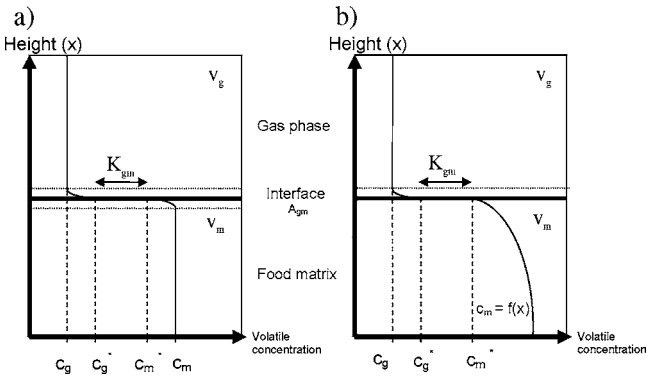

Figure 1. Schematic representation of aroma profiles during release from the matrix to the gas phase. (**a**) Convective transfer mechanisms in matrix and in gas phases. (**b**) Diffusive transfer mechanism in the matrix phase and convective mechanism in the gas phase.

(**Figure 1b**). When the matrix phase is well-stirred (**Figure 1a**), the aroma compound concentration is the same in the whole food matrix (no concentration gradient) except in a thin boundary layer near the surface. When the matrix phase is not stirred, the establishment of gradient concentration in the matrix is observed (**Figure 1b**). In the gas phase, volatile transport is much faster than in liquid and solid samples and the concentration gradient is generally neglected, with the possible exception of the thin boundary layer near the interface (**Figure 1a**,**b**).

In this paper, a model corresponding to mass transfer in an unstirred closed system was developed. The aim was to identify physical properties of the aroma compound−matrix couple responsible for aroma release, independently of the experimental setup. Juteau et al. (*14*) have previously used a convective model to describe aroma release from water, thickened, and gelled matrices. These authors showed that there was a gap between experimental and modeled data and explained these differences by the establishment of a gradient concentration in the matrix. Using their experimental data (previously published and new data), we developed a diffusive model, taking into account the concentration gradient between the bulk phase and the surface layer.

MATERIALS AND METHODS

Mechanism Modeling. Depending on hydrodynamic conditions, the volatile compound mass transfer may be described by a convective or diffusive mass transfer model.

Convective Mass Transfer Model. The convective model used was developed by Harrison and Hills (*20*, *21*). One major hypothesis concerning the convective model was that the concentration of the volatile compounds in the gas and the product phases is homogeneous at any given time, except for a very thin boundary layer. Therefore, convection was assumed to be the main physical phenomenon in the matrix phase, as schematically shown in **Figure 1a**. These authors also neglected the mass transfer resistance in the boundary layer of the gas phase, thus assuming perfectly uniform gas concentrations ($C_g = C_g^*$ in **Figure 1a**).

Diffusive Mass Transfer Model. A mechanistic model was set up to determine both diffusion and partition coefficients of aroma compounds in solutions and hydrogels. The entire experimental protocol was taken into account for the model development, including the first equilibration (step 1), the purge step (step 2), and the volatile compound release (step 3), as described in the experimental section. Several assumptions based on the experimental setup are given below.

In the Matrix Phase. First, the matrix is not stirred. Thus, the compound transfer in this phase is best described as a diffusive transport (**Figure 1b**). Because of the horizontal plane symmetry, only one-dimensional transport along the vertical axis (0x) is considered. According to the second Fick's law, the volatile concentration in the matrix phase depends on the vertical position and is given by:

$$\frac{\partial c_m(x,t)}{\partial t} = D_m \cdot \frac{\partial^2 c_m(x,t)}{\partial x^2} \quad (1)$$

with $x \in [0,L]$ and $t \geq t_0$, where t_0 corresponds to the beginning of step 1 of the experiment (−122 min).

Second, with regard to boundary conditions, the volatile compound flux is zero at the bottom of the vial, which is expressed as:

$$\frac{\partial c_m(0,t)}{\partial x} = 0 \quad (2)$$

At the product−air interface, the mass flux conservation is written as:

$$-D_m \cdot \frac{\partial c_m(L,t)}{\partial x} = k_g \cdot [c_g^*(t) - c_g(t)] \quad (3)$$

Third, the initial volatile compound concentration in the matrix is supposed to be uniform. Indeed, volatile compounds are introduced into the food matrix and the bottle is immediately sealed and stirred for 15 s. The bottle is then placed in a bath at 30 °C. At this moment, the volatile compound concentration is assumed to be the same throughout the whole matrix. This can be written as:

$$c_m(x,t_0) = c_{m0} \quad (4)$$

with $x \in [0,L]$.

Partitioning at the Gas−Matrix Interface. At the gas−matrix interface, local thermodynamic equilibrium is assumed at any given time. The volatile compound concentration ratio between the gas phase at the interface $c_g^*(t)$ and the matrix phase at the interface $c_m^*(t)$ is equal to the partition coefficient of the volatile compound:

$$\frac{c_g^*(t)}{c_m^*(t)} = K_{gm} \quad (5)$$

In the Gas Phase. In the gas phase, diffusion coefficients are about 10000 times higher than in the matrix (*22*), suggesting that the gradient concentration in the headspace can be ignored, except in the thin boundary layer as shown in **Figure 1b**. Changes in aroma compound concentrations in the gas phase can be described on the basis of a mass balance for the experimental system when $t \geq t_0$, using a mass transfer coefficient in the boundary layer of the gas phase (convective mechanism) as follows:

$$V_g \cdot \frac{dc_g(t)}{dt} = k_g \cdot A_{gm} \cdot [c_g^*(t) - c_g(t)] - Q_g(t) \cdot c_g(t) \quad (6)$$

During steps 1 and 3, the system is closed and the air flow rate $Q_g(t)$ is equal to zero. During the purge step (step 2), the system is opened and a 500 mL min^{-1} air flow is introduced. Losses induced by this flow $Q_g(t)$ are taken into account in the mass balance equation for step 2.

Moreover, concerning the initial conditions of the experiment, it was assumed that no aroma compound was present in the gas phase until the beginning of step 1:

$$c_g(t_0) = 0 \quad (7)$$

Numerical Resolution. A spatial discretization of the partial differential equation (eq 1) using the finite volume method (*23*) was performed. The product was divided into N virtual layers of length L_m. The centers of the finite volumes are represented by the dashes on the vertical axis of **Figure 2**. The mass balance in each layer (the elementary volume $L_m \cdot A_{gm}$) is

$$\text{accumulation rate in an elementary volume} = \text{(incoming flux)} - \text{(outgoing flux)} \quad (8)$$

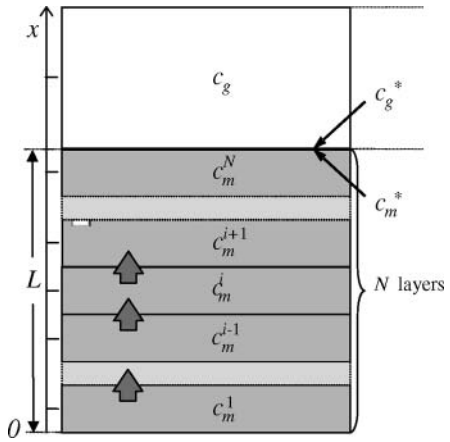

Figure 2. Spatial discretization for solving the partial differential equation according to the finite volume method; in gray, the food matrix; in white, the gas phase.

The general equation is applied to the N theoretical layers of the product where i corresponds to the layer number:

$$A_{gm} \cdot L_m \cdot \frac{dc_m^i}{dt} = A_{gm} \cdot D_m \cdot \left(\frac{c_m^{i-1} - c_m^i}{L_m}\right) - A_{gm} \cdot D_m \cdot \left(\frac{c_m^i - c_m^{i+1}}{L_m}\right) \quad (9)$$

Special forms of this equation were written for the first layer (near the vial bottom) and the last layer (near the product interface) in order to take boundary conditions into account (eqs 2 and 3).

Composition and Preparation of Flavored Polysaccharide Matrices. Three different concentrations of NaCl were chosen to generate three different melting temperatures of 1% ι-carrageenan matrices. The three matrices exhibited three different rheological behaviors at 30 °C as previously described (*14*): a macromolecular solution behavior (0.1% NaCl w/w), a very soft gel (0.3% NaCl w/w), and a relatively hard one (0.5% NaCl w/w).

The method was already presented in detail in Juteau et al. (*14*). Samples (24 mL flavored matrices in 100 mL borosilicate vials) were done in triplicate. The flavored carrageenan matrices were prepared by mixing carrageenans in salted aqueous solutions at 20 °C. The mixture was then stirred at 90 °C for 30 min for a complete solvation of all macromolecular chains. Reference solutions containing the same amount of salt and replacing the hydrocolloid by an equal mass of pure water were also flavored and analyzed.

Ethyl hexanoate is a frequently used compound in food aroma formulation. Ethyl hexanoate was added after the matrices were cooled from 90 to 60 °C. The concentration was set to 10 μL L^{-1} corresponding to 8.73×10^3 mg m^{-3}. The volatile compound losses during the preparation of the sample were estimated by CH_2Cl_2 extraction with the experimental procedure described in ref *14*.

Samples were then equilibrated for 2 h at 30 °C without stirring (step 1 of the experiment). This first step was initially intended to obtain a thermal and physical equilibrium between the two phases. To begin kinetic measurements with the lowest possible aroma concentration in the headspace, the gas phase in the vial was renewed with a 500 mL min^{-1} air flow for 2 min (step 2 of the experiment). The same procedure was applied to the reference solutions (without polysaccharides).

Static Headspace Analysis. The analyzed matrices were maintained at 30 °C for different times (5−7200 s) (step 3 of the experiment). Only one sample per flask was analyzed. Vapor-phase samples (1 mL) were manually taken with a gastight syringe (1 mL, SGE) and manually injected into a HP 6890 gas chromatograph at the following times: 8.3×10^{-2}, 3, 5, 7, 30, 120, and 240 min.

Diffusive Model Fitting. The differential algebraic equations (eqs 1−9) system was solved using Matlab 7 (The MathWorks, MA). The unknown parameters (K_{gm} and D_m) were adjusted to the experimental gaseous concentration C_g using the Levenberg−Marquardt method of minimization of the least-squares norm.

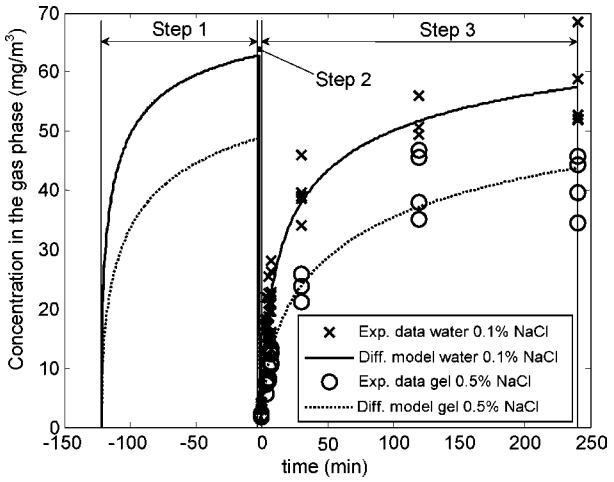

Figure 3. Gas-phase concentration profile of ethyl hexanoate during the whole release experiment from water (0.1% NaCl) and from 1% ι-carrageenan gel (0.5% NaCl), including the three experimental steps. Step 1, 2 h at 30 °C under static conditions; step 2, purge of the headspace; and step 3, kinetics of the release under static conditions at 30 °C. The origin of the time scale corresponds to the beginning of the release step of the experiment (step 3).

The confidence interval for the partition coefficient K_{gm} (and similarly for D_m) was determined as:

$$K_{min/max} = K_{gm} \pm t_{(1-\alpha)/2,\upsilon} \cdot \sigma_K \quad (10)$$

where $t_{(1-\alpha)/2,\upsilon}$ is the inverse of the Student cumulative distribution at confidence level α and υ degrees of freedom. The confidence level was selected as $\alpha = 0.95$, and the number of degrees of freedom was $\upsilon = M - 2$ since two parameters (K_{gm} and D_m) were determined from M measurements. The standard error σ_K was determined from the so-called local information matrix, computed during the model fitting step (*24*).

RESULTS AND DISCUSSION

Concentration Profiles in the Gas Phase during Release Measurements. As an example, **Figure 3** shows the time-dependent release curve of ethyl hexanoate from salted water with 0.1% NaCl and from a 1% ι-carrageenan gel with 0.5% NaCl. The curve consists of three distinguishable parts corresponding to the three steps of the experiment. Step 1 begins at the initial time of the experiment, whereas step 3 begins at the initial time of the measured release step. Step 2 refers to the purge time between the two. Similar curves were obtained for ethyl hexanoate from salted water with 0.5% NaCl and from 1% ι-carrageenan matrices containing 0.1, 0.3, and 0.5% of sodium chloride.

Step 1 corresponds to the first equilibration at 30 °C for 2 h. No experimental data were obtained for this part, and the bold curve corresponds to simulated concentrations of the volatile compound in the gas phase. This concentration increases rapidly during the first 20 min, then the increase rate gradually slows down, and the headspace concentration at 120 min is close to 65 mg m^{-3}. **Figure 3** shows that perfect equilibrium was not actually reached at the end of step 1, as assumed in the previous work (*16*).

In step 2, the model simulates the gas-phase renewal by a 500 mL min^{-1} gas flow for 2 min. As expected, the volatile compound concentration in the gas phase decreases rapidly. At the end of the purge, the concentration of the volatile compound in the gas phase is very low but not null. It is close to

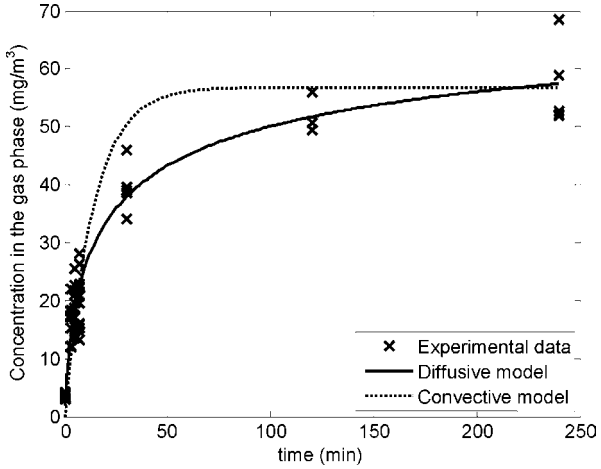

Figure 4. Comparison of diffusive and convective release models to experimental data of ethyl hexanoate release from water with 0.1% NaCl at 30 °C.

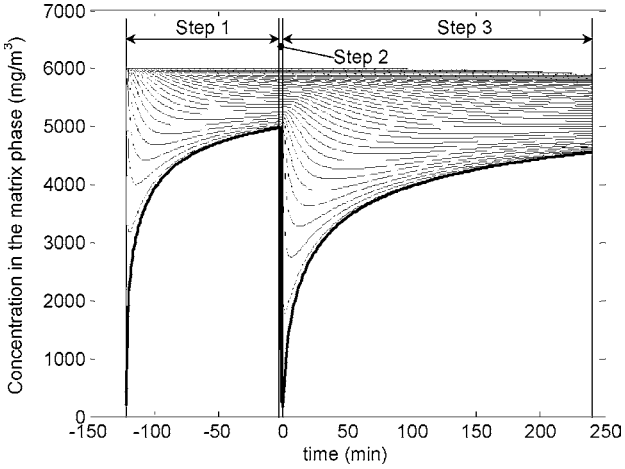

Figure 5. Calculated concentration profile for ethyl hexanoate in water with 0.1% NaCl. Thin curves, volatile concentration in the different layers in the bulk phase; bold curve, volatile concentration at the interface. The origin of the time scale corresponds to the beginning of the release step of the experiment (step 3).

1.26 mg m^{-3}. Thus, this simulated step provides missing information since it is experimentally very difficult to measure the initial concentration of the volatile compound at the beginning of the volatile compound release curve (step 3).

During step 3, the gas flow was stopped and the volatile compound concentration in the gas phase increased. The initial high rate of release slows down progressively and the concentration in the gas phase tends to an equilibrium value, depending on the partition coefficient of ethyl hexanoate in the considered experimental conditions (matrices, pressure, and temperature). This part is the only one experimentally determined. Experimental values are represented as symbols. **Figure 3** shows fair agreement between experimental and modeled data, regardless of the matrix, which shows that the selected diffusive model is appropriate for the description of the considered experimental setup.

Comparison with Previous Results Obtained with a Convective Model of Volatile Compound Release. Figure 4 shows the adjustment of the diffusive model and of the previous convective model to the experimental data obtained with salted water. Both have the same slope rate at initial time. The values of the calculated parameters (partition and diffusion coefficients) are discussed in the next sections.

With the previous approach (convective model), a deviation between theoretical and experimental points was observed in the middle section of the curve (**Figure 4**). Such a deviation has already been reported for stirred matrices (*25*, *13*). When experimental concentrations in the central part of the release curve were systematically higher than model predictions, this was explained by an increased exchange area due to a high stirring rate. The opposite situation was explained in ref *11* by an inefficient stirring, that is, the establishment of a concentration gradient between the surface layer and the bulk of the matrix. For the considered unstirred systems, this assumption was confirmed by the calculation of the apparent order of the release kinetic (*16*, *19*).

In contrast, the product concentration is not assumed to be homogeneous with the diffusive model, and the establishment of the gradient can be simulated and taken into account during the whole experiment. Indeed, with the current approach, the theoretical volatile compound concentration depends on the position in the matrix. **Figure 5** represents the calculated time-dependent concentrations at several locations in the food matrix. The most concentrated layers are located at the bottom of the vial. The bold line represents the volatile concentration in the matrix at the interface (c_m^*) and is equal to the gas concentration at the interface divided by the partition coefficient, as given by eq 5. Moreover, the time-dependent concentration in various locations in the product was also simulated for steps 1 and 2. According to **Figure 3**, the concentration at initial time (beginning of step 1) is assumed to be null in the gas phase and homogeneous in the product because it was vigorously stirred. The aroma concentration in the very first layers of product located near the interface decreases quickly, while the volatile compound concentration in the gas phase increases. These first matrix layers are drained, but the concentration in the deeper layers does not considerably vary because of the low diffusion coefficient and the relatively short duration of the experiment (400 min).

On the basis of the same experimental data, such as those in **Figure 4**, the estimations of the partition coefficients are slightly different depending on which transfer mechanism is assumed in the matrix, either convective or diffusive. According to the convective hypothesis, equilibrium is reached within the duration of the experiment, while according to the diffusive hypothesis, it is not (**Figure 4**). With the convective model, the last experimental points (240 min) correspond to equilibrium partitioning, while with the diffusive model, these last points still correspond to a transient (increasing) regime, the equilibrium concentration being higher. The estimated partition coefficients are thus slightly higher with the diffusive model. These estimations are preferred because the diffusive mechanism better corresponds to the physical reality of the considered experiments (unstirred and, in some cases, thickened or gelled matrices).

Estimation of the Thermodynamic and Kinetic Parameters. *Partition Coefficient Determination.* **Figure 6** gives the partition coefficients determined using both convective and diffusive models for ethyl hexanoate in water (0.1 and 0.5%) and in 1% ι-carrageenan matrices containing 0.1, 0.3, and 0.5% NaCl.

The partition coefficient of ethyl hexanoate in water determined using the diffusive model (12.6×10^{-3} in water with 0.1% NaCl, 30 °C) is slightly lower but in the same range as those found in the literature. Indeed, relatively large differences can be found between partition coefficients when measured by

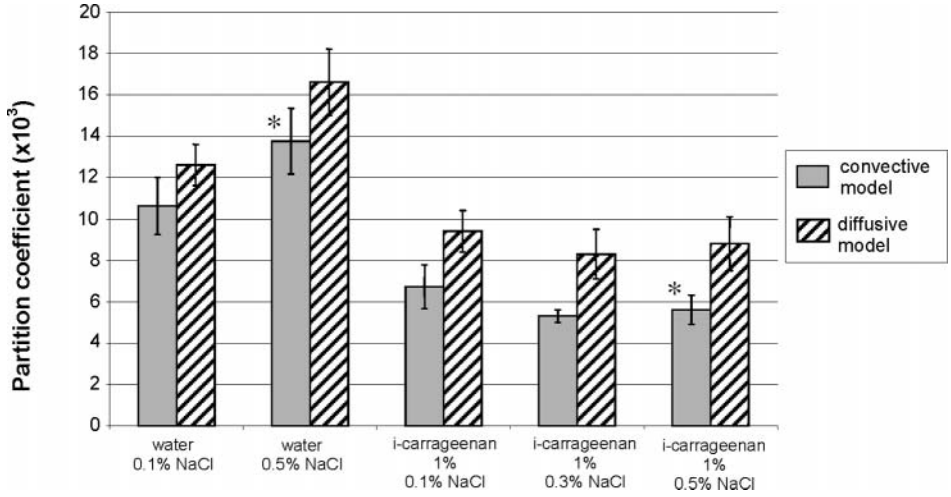

Figure 6. Partition coefficients of ethyl hexanoate estimated with the convective and the diffusive models in water (0.1 and 0.5% NaCl) and 1% ι-carrageenan matrices (0.1, 0.3, and 0.5% NaCl) at 30 °C. Error bars correspond to the 95% confidence interval; *, data from ref *16*.

different methods (*26*). For example, the partition coefficient of ethyl hexanoate obtained by van Ruth et al. (*27*) at 25 °C in water was 34×10^{-3} by static headspace analysis, whereas the partition coefficient calculated from the activity coefficient at infinite dilution and the saturated vapor pressure measured by Le Than et al. (*28*) was 18×10^{-3} under the same conditions (25 °C). The partition coefficient estimated with the diffusive model is 18% higher than the partition coefficient previously calculated with the convective model using the same data set. Thus, it is closer to the values found in the literature. On the basis of the 95% interval confidence, this difference is not significant for ethyl hexanoate in salted aqueous solutions. For polysaccharidic matrices, the partition coefficient is around 50% higher using the diffusive model (for 0.1−0.5% NaCl matrices, respectively). For these systems, the differences between the partition coefficients estimated with the two approaches are significant (based on 95% confidence intervals).

Partition coefficients calculated with the two models for ethyl hexanoate in 1% ι-carrageenan matrices are significantly lower than those calculated for ethyl hexanoate in water, suggesting molecular interactions between the ester and the polysaccharidic chains. This was also observed for ethyl butanoate, another ester, but not for linalool (*14*).

For ethyl hexanoate in water, a significant increase of the partition coefficient was observed when NaCl concentration increased. This can be explained by changes in the activity coefficient of the volatile compound (*29*). This salting-out effect was also observed using the convective model. However, in the three polysaccharidic matrices, no significant differences were obtained between the thickened solution (0.1% NaCl), the soft gel (0.3% NaCl), and the hard gel (0.5% NaCl). The salting-out effect may have been concealed by an increased retention when the degree of structuring was increased.

Moreover, the more structured the matrix is, the more the differences between the two estimated partition coefficients increase. An explanation is that slower transfer in structured matrices implies that the system is farther from equilibrium at the final time of the experiment, implying larger differences between the two estimation of the partition coefficient, as mentioned above.

Diffusion Coefficient Determination. Fitting the diffusive model parameters to the experimental data allows the determination of the diffusion coefficients of ethyl hexanoate in the different matrices at 30 °C (**Table 1**).

Table 1. Diffusion Coefficients of Ethyl Hexanoate in H_2O and ι-Carrageenan Matrices at 30 °C[a]

	H_2O		1% ι-carrageenan		
	+0.1% NaCl	+0.5% NaCl	+0.1% NaCl	+0.3% NaCl	+0.5% NaCl
D_m (10^{-10} m^2 s^{-1})	8.5	8.5	1.6	1.7	1.3
CV (%)	9.5	11.8	11.5	18.5	20.8

[a] Determination by fitting the diffusive model parameters to experimental data.

Considering the salted solutions, the ethyl hexanoate diffusion coefficient was estimated at 8.5×10^{-10} m^2 s^{-1} with coefficients of variation between 9 and 12%. An increase in salt concentration from 0.1 to 0.5% did not induce any change in the diffusion coefficient. Taking the variability of the headspace analysis and the structure of the experimental data set into account, these results can be considered as accurate estimations. A comparison with the values available in the literature (estimated with empirical equations or experimentally measured) also confirmed their reliability, even if it was the diffusion of ethyl hexanoate in pure water that was considered (**Table 2**). The absence of salt effect on diffusion was also measured by NMR spectroscopy concerning the diffusion of ethyl guaicol in salted solutions from 0.1 to 0.3% NaCl (**Table 3**; *30*).

Regardless of the salt concentration (0.1 or 0.5%), the addition of 1% ι-carrageenan induces at least a five-fold decrease of the diffusion coefficient of ethyl hexanoate (**Table 1**). Our previous determination obtained with the convective model highlighted a similar effect on the mass transfer coefficient (*14*). This can be explained by an increased viscosity, as predicted by the Stoke−Einstein equation. The study of ethyl guaicol diffusion in 1% ι-carrageenan matrices by NMR with 0.1 or 0.3% NaCl also highlighted a 1.7-fold decrease of the aroma diffusion in the gel as compared to the free solution (**Table 3**; *30*). Because no chemical interaction or obstruction effects were identified, these authors suggested that this retardation of the aroma compound diffusion could originate from frictional effects (incomplete gelation under these conditions, leading to a heterogeneous system).

In polysaccharide gels, the effect of an increase in salt concentration on the diffusion coefficients remains limited in our study, even if we can observe a 20% decrease when NaCl concentration reaches 0.5% (**Table 1**). It is known that an

Table 2. Diffusion Coefficients of Ethyl Hexanoate in H_2O or D_2O[a]

	experimental values		estimated values	
medium	H_2O	D_2O	H_2O	H_2O
temperature (°C)	25	30	30	30
method	Stokes cell	NMR DOSY	Wilke and Chang equation	Hayduk–Minas equation
D_m (10^{-10} m^2 s^{-1})	7.9 (CV < 10%)	8.5 (CV < 5%)	8.14	7.13
refs	*35*	*36*	*37*	*37*

[a] Experimental or calculated values found in the literature.

Table 3. Diffusion Coefficients of Ethyl Guaicol (*30*) and Ethyl Butanoate (*33*) in H_2O and ι-Carrageenan Matrices at 30 °C[a]

D_m (10^{-10} m^2 s^{-1})		0.1% NaCl	0.3% NaCl	0.5% NaCl
		ethyl guaicol[b,d]		
ι-carrageenan concentration (%)	H_2O	8.2	7.6	
	1%	4.8	4.8	
	2%	5.8	5.6	
		ethyl butanoate[c,d]		
	1%	8.71 (±0.76)	9.37 (±0.24)	10.04 (±0.65)

[a] Determination by ^{1}H NMR DOSY. [b] Standard deviations were estimated for the diffusion coefficients between 0.01 and 0.05. [c] Values are means (±confidence intervals at 95%). [d] Diffusion coefficient of ethyl gaicol and ethyl butanoate in water at 30 °C calculated from the Wilke and Chang (*34*): $D_{EG,30°C} = 8.5 \times 10^{-10}$ m^2 s^{-1} and $D_{EB,30°C} = 9.4 \times 10^{-10}$ m^2 s^{-1}, respectively.

increase of salt concentration leads first to the formation of the carrageenan network (up to 0.3%) and then to a more rigid gel (up to 0.5%) (*14*). These results suggest that the effect of the addition of 1% polysaccharide on diffusion is much more important than the subsequent structuring of the macromolecular chains in a three-dimensional network. Rondeau-Mouro et al. (*30*) came to the same conclusions for ethyl guaicol diffusion in 1 or 2% ι-carrageenan gels since no salt effect was identified. This preponderant effect of the addition of the polysaccharides can be related to the modification of the dry matter content, known to greatly influence aroma compound mobility (*31*).

Yet, Colsenet et al. (*32*) obtained a faster diffusion for biggest PEGs in casein gels than in casein solutions. This effect was not identified for PEGs with lower molecular weight. Gostan et al. (*33*) showed a 13% increase of the diffusion coefficient of ethyl butyrate in 1% ι-carrageenan gels for NaCl content varying from 0.1 to 0.5% (**Table 3**). Even if these variations remain limited, they suggested a positive effect of a better structured network, leading to an increase in the open space available for molecular movements of the free molecules. The comparison of experimental values of diffusion coefficients of ethyl butanoate (*33*) with calculated value ($D_{EB,30°C} = 9.4 \times 10^{-10}$ m^2 s^{-1}) on the basis of Wilke's and Chang's equation (*34*) confirmed that this structuring effect remains limited.

This macroscopic study allows the determination of the diffusion coefficient of aroma compounds independently from the experimental setup. Comparisons with the literature demonstrated the reliability of the approach. It appeared that in ι-carrageenan gels, the aroma compounds mobility is more or less limited by the level of the matrix organization and seems to essentially diffuse through the free phase (water).

It was observed in this study that the addition of 1% carrageenan induced a higher reduction (5.3-fold) in the diffusion coefficient with regard to the results of Rondeau-Mouro et al. (*30*) (1.7-fold decrease). This could be attributed to the existence of molecular interactions between ethyl hexanoate and polysaccharides chains (since a decrease in the partition coefficient in gels was obtained). However, we can also suggest that this discrepancy could originate from the observation scale: with NMR measurements, local diffusion in the bulk phase is considered, whereas our methodology results in a macroscopic analysis, leading to the determination of an apparent diffusion coefficient.

Concerning NMR measurements, we can observe that the use of D_2O is known to modify the rheological properties of matrices, leading to more rigid gels (*30*). One can also question the effect that the small size of the NMR cell has on gel formation.

With the objective of a better understanding of aroma compound release in relation to sensory perceptions, the considered methodology seems to be more appropriate for complex food matrices containing numerous aroma compounds.

Influence of the Modeling Assumptions on the Determined Partition and Diffusion Coefficient Values. For accurate determination of the partition and diffusion coefficients using the described method, modeling assumptions must closely reflect the actual experimental protocol. The effects of some of these assumptions are presented below.

Initial Volatile Compound Concentration in the Product and Measured Headspace Concentration. The dynamic model of the aroma release strongly relies on the mass balance of the aroma compound between the product and the headspace. Possible errors in the initial aroma concentration in the product or in the measured concentration in the headspace significantly affect the determination of the partition and diffusion coefficients. For example, overestimating the initial product concentration by 20% in the case of a 0.1% NaCl solution would result in a 19% underestimation of the partition coefficient and a 29% underestimation of the diffusion coefficient. Such situations are likely to arise in practice, for example, if volatile compound losses during matrix preparation are not taken into account. It is thus important to verify the actual aroma concentration in the product before the beginning of the experiment, especially when working with highly volatile compounds at high temperatures. Systematic errors in the measured headspace concentration, due, for example, to gas chromatograph calibration, have similar effects.

Equilibration Step. The experimental protocol includes a 2 h equilibration step. Simulations show that complete equilibrium is not actually reached in this step: Some concentration gradient still exists in the product, and the gas concentration is not perfectly constant (**Figure 3**). The system is sufficiently close to equilibrium, however, for the exact duration of the equilibration step to have relatively little effect on the determined partition and diffusion coefficient values. For example, a 20% overestimation of this duration does not change the determined partition coefficient and underestimates the diffusion coefficient by less than 4%. However, modeling this step in the experimental protocol is important. Fitting a simplified model (without the equilibration step) to the experimental data would result in a 25% underestimation of the diffusion coefficient.

Purge Step. During the purge step, a strong aroma concentration gradient is created in the superficial product layer, which influences subsequent aroma release during the headspace concentration measurement step. Simulations show that overestimating the purge duration or the purge flow rate by 20% has a negligible effect on the determined partition coefficient and overestimates the diffusion coefficient by 15 and 5%, respectively. This is relatively low as compared to the overall uncertainty in the determined value of the diffusion coefficient, as indicated by its variation coefficient (**Table 1**). Exact knowledge of the experimental conditions during the purge step is therefore not critical. Not to model the purge step completely would be an unacceptable approximation, however. Indeed, fitting a simplified model (without the purge step) to the experimental data would result in a 75% underestimation of the diffusion coefficient.

In conclusion, the determination of the partition and of the diffusion coefficients by the considered method relies on an accurate modeling of the various phases of the experimental protocol, including equilibration and purge. The determination of the diffusion coefficient appears to be the most sensitive to true experimental conditions. The most important conditions turn out to be the initial aroma concentration in the product and the calibration of the gas chromatograph. Taking these important points into account, it is possible to determine some specific physicochemical parameters of the solute in the matrix, even for complex real matrices that could not be studied by other expensive direct measurements methods, using just a simple experimental apparatus combined with a mechanistic modeling approach. The knowledge of these physicochemical parameters will be necessary for the description of aroma release mechanisms in food preparation, storage, and consumption conditions.

ABBREVIATIONS USED

A_{gm}, gas−liquid contact area (17.9×10^{-4} m^2); $c_g(t)$, volatile concentration in the gas phase (mg/m^3); $c_g^*(t)$, interfacial volatile concentration in the gas phase (mg/m^3); $c_m(0)$, initial volatile concentration in the matrix phase (mg/m^3); $c_m(t)$, volatile concentration in the matrix phase (mg/m^3); $c_m^*(t)$, interfacial volatile concentration in the matrix phase (mg/m^3); D_m, matrix phase diffusion coefficient (m^2/s); k_g, mass transfer coefficient in the gas phase (3×10^{-2} m/s); K_{gm}, gas−matrix partition coefficient; L, height of the matrix phase (1.35×10^{-2} m); N, number of theoretical layers in the matrix phase ($N = 100$); Q_g, gas flow rate (8.3×10^{-6} m^3/s); t, time (s); t_0, beginning of step 1 (−7320 s); v_m, volume of matrix phase (24×10^{-6} m^3); v_g, volume of gaseous phase (111.6×10^{-6} m^3).

LITERATURE CITED

(1) Guichard, E. Interactions between flavor compounds and food ingredients and their influence on flavor perception. *Food Rev. Int.* **2002**, *18*, 49−70.

(2) Baines, Z. V.; Moris, E. R. Flavour/taste perception in thickened systems: The effect of guar gum above and below C*. *Food Hydrocolloids* **1987**, *1*, 197−205.

(3) Wendin, K.; Solheim, R.; Allmere, T.; Johanson, L. Flavour and texture in sourmilk affected by thickeners and fat content. *Food Qual. Pref.* **1997**, *8*, 281−291.

(4) Hollowood, T. A.; Lindforth, R. S. T.; Taylor, A. J. The effect of viscosity on the perception of flavor. *Chem. Senses* **2002**, *27*, 583−591.

(5) Weel, K. G. C.; Boelrijk, A. E. M.; Alting, A. C.; vanMil, P. J. J. M.; Burger, J. J.; Gruppen, H.; Voragen, A. G. J.; Smit, G. Flavor release and perception of flavored whey protein gels: Perception is determined by texture rather than by release. *J. Agric. Food Chem.* **2002**, *50*, 5149−5155.

(6) Boland, A. B.; Delahunty, C. M.; van Ruth, S. M. Influence of texture of gelatin gels and pectin gels on strawberry flavor release and perception. *Food Chem.* **2006**, *96*, 452−460.

(7) Saint-Eve, A.; Martin, N.; Guillemin, H.; Semon, E.; Guichard, E.; Souchon, I. Flavored stirred yogurts structure affects the real-time aroma release and the temporal sensory properties during eating. *J. Agric. Food Chem.* **2007**, in press.

(8) Baek, I.; Linforth, R. S. T.; Blake, A.; Taylor, A. J. Sensory perception is related to the rate of change of volatile concentration in-nose during eating of model gels. *Chem. Senses* **1999**, *24*, 155−160.

(9) Taylor, A. J.; Linforth, R. S. T.; Harvey, B. A.; Blake, A. Atmospheric pressure chemical ionisation mass spectrometry for *in vivo* analysis of volatile flavor release. *Food Chem.* **2000**, *71*, 327−338.

(10) Hansson, A.; Giannouli, P.; van Ruth, S. The influence of gel strength on aroma release from pectin gels in a model mouth and *in-vivo*, monitored with proton-transfer-reaction mass spectrometry. *J. Agric. Food Chem.* **2003**, *51*, 4732−4740.

(11) Andriot, I.; Harrison, M.; Fournier, N.; Guichard, E. Interactions between methyl ketones and β-lactoglobulin: Sensory analysis, headspace analysis, and mathematical modeling. *J. Agric. Food Chem.* **2000**, *48*, 4246−4251.

(12) van Ruth, S. M.; Roozen, J. P. Influence of mastication and saliva on aroma release in a model mouth system. *Food Chem.* **2000**, *71*, 339−345.

(13) Marin, M.; Baek, I.; Taylor, A. J. Volatile release from aqueous solutions under dynamic headspace dilution conditions. *J. Agric. Food Chem.* **1999**, *47*, 4750−4755.

(14) Juteau, A.; Doublier, J.-L.; Guichard, E. Flavor release from ι-carrageenan matrices: A kinetic approach. *J. Agric. Food Chem.* **2004**, *52*, 1621−1629.

(15) Linforth, R. S. T. Modeling flavor release. In *Food Flavor Technology*; Taylor, A. J., Ed.; Sheffield Academic Press Ltd.: Sheffield, 2002; pp 185−209.

(16) Juteau, A.; Cayot, N.; Chabanet, C.; Doublier, J.-L.; Guichard, E. Flavor release from polysaccharide gels: Different approaches for the determination of kinetic parameters. *Trends Food Sci. Technol.* **2004**, *15*, 394−402.

(17) Tromelin, A.; Hautbout, G.; Pourcelot, Y. Application of fractal geometry to dissolution kinetic study of a sweetener excipient. *Int. J. Pharm.* **2001**, *224*, 131−140.

(18) Harrison, M.; Hills, B. P. Mathematical model of flavor release from liquids containing aroma-binding macromolecules *J. Agric. Food Chem.* **1997**, *45*, 1883−1890.

(19) Cussler, E. L. In *Diffusion. Mass Transfer in Fluid Systems*, 2nd ed.; University Press: Cambridge, 1997.

(20) Harrison, M.; Hills, B. P.; Bakker, J.; Clothier, T. Mathematical models of flavor release from liquid emulsions. *J. Food Sci.* **1997**, *62*, 653−658, 664.

(21) Harrison, M.; Hills, B. P. Effects of air flow-rate on flavor release from liquid emulsions in the mouth. *Int. J. Food Sci. Technol.* **1997**, *32*, 1−9.

(22) Gascons-Viladomat, F.; Souchon, I.; Athès, V.; Marin, M. Membrane air-stripping of aroma compounds. *J. Membr. Sci.* **2006**, *277*, 129−136.

(23) Crank, J. In *The Mathematics of Diffusion*, 2nd ed.; Clarendon Press: Oxford, 1975.

(24) Bury, K. In *Statistical Distributions in Engineering*; Cambridge University Press: Cambridge, 1999.

(25) Bakker, J.; Boudaud, N.; Harrison, M. Dynamic release of diacetyl from liquid gelatin in the headspace. *J. Agric. Food Chem.* **1998**, *46*, 2714−2720.

(26) Athès, V.; Pena y Lillo, M.; Bernard, C.; Perez, R.; Souchon, I. Comparison of experimental methods for measuring infinite dilution volatilities of aroma compounds in water / ethanol mixtures. *J. Agric. Food Chem.* **2004**, *52*, 2021−2027.

(27) van Ruth, S. M.; de Vries, G.; Geary, M.; Giannouli, P. Influence of composition and structure of oil-in-water emulsions on retention of aroma compounds. *J. Sci. Food Agric.* **2002**, *82*, 1028−1035.

(28) Le Thanh, M.; Lamer, T.; Voilley, A.; Jose, J. Détermination des coefficients de partage vapeur-liquide et d'activité de composés d'arôme à partir de leurs caractéristiques physico-chimiques. *J. Chem. Phys.* **1993**, *90*, 545−560.

(29) Voilley, A.; Simatos, D.; Loncin, M. Gas phase concentration of volatiles in equilibrium with a liquid aqueous phase. *Lebensm. Wiss. Technol.* **1977**, *10*, 45−49.

(30) Rondeau-Mouro, C.; Zykwinska, A.; Durand, S.; Doublier, J.-L.; Buleon, A. NMR investigations of the 4-ethyl guaicol self-diffusion in ι-carrageenan gels. *Carbohydr. Polym.* **2004**, *57*, 459−468.

(31) Voilley, A.; Souchon, I. Flavor retention and release from the food matrix: an overview. In *Flavor in Food*; Voilley, A., Etiévant, P., Eds.; Woodhead Publishing Ltd.: Cambridge, 2006.

(32) Colsenet, R.; Soderman, O.; Mariette, F. Diffusion of polyethyleneglycols in casein solutions and gels studied by pulsed field gradient NMR. *Magn. Reson. Chem.* **2005**, *42*, 496−499.

(33) Gostan, T.; Moreau, C.; Juteau, A.; Guichard, E.; Delsuc, M. A. Measurement of aroma compound self-diffusion in food models by DOSY. *Magn. Reson. Chem.* **2004**, *42*, 496−499.

(34) Wilke, C. R.; Chang, P. Correlation of diffusion coefficients in dilute solutions. *AIChE J.* **1955**, *1* (2), 264−270.

(35) Lamer, T. Extraction de composés d'arôme par pervaporation. Relation entre les propriétés physico-chimiques des substances d'arômes et leur transfert à travers des membranes à base de polydiméthylsiloxane. Ph.D. Thesis, University of Burgundy, France, 1993.

(36) Savary, G.; Guinee, T. P.; Doublier, J.-L.; Cayot, N.; Moreau, C. Influence of ingredients on the self-diffusion of aroma compounds in a model fruit preparation: A nuclear magnetic resonance-diffusion-ordered spectroscopy investigation. *J. Agric. Food Chem.* **2006**, *54*, 665−671.

(37) Reid, R. C.; Prausnitz, J. M.; Poling, B. E. In *The Properties of Gases and Liquids*, 4th ed.; MacGraw-Hill Book Co.: New York, 1987.

Received for review September 15, 2006. Revised manuscript received March 7, 2007. Accepted March 10, 2007. This work was supported by the French government within the framework of the CANAL-ARLE project.

JF0626415